Editors' Suggestion

High Phase-Purity and Composition-Tunable Ferromagnetic Icosahedral Quasicrystal

Ryo Takeuchi,[1,*] Farid Labib,[1,*] Takafumi Tsugawa,[1] Yuto Akai,[1] Asuka Ishikawa,[2] Shintaro Suzuki,[1] Takenori Fujii,[3] and Ryuji Tamura[1,†]

[1]*Department of Materials Science and Technology, Tokyo University of Science, Tokyo 125-8585, Japan*
[2]*Research Institute of Science and Technology, Tokyo University of Science, Tokyo 125-8585, Japan*
[3]*Cryogenic Research Center, The University of Tokyo, Bunkyo, Tokyo 113-0032, Japan*

(Received 14 November 2022; accepted 27 March 2023; published 26 April 2023)

We discovered a ferromagnetic Au-Ga-Dy icosahedral quasicrystal (*i* QC), not only with high phase purity but also with tunable composition. The isothermal magnetization of the polycrystalline ferromagnetic *i* QC was closely investigated and the mean-field-like nature of the ferromagnetic transition is elucidated. Moreover, the maximum Weiss temperature (θ_p) of the *i* QCs was found at the electrons-per-atom (e/a) ratio of 1.70 being well consistent with those of ACs, validating tunability of the magnetic properties of *i* QCs on the basis of $\theta_p - e/a$ scheme for the first time. Thus, the present work provided direct evidence that the magnetism of the *i* QCs depends on the e/a ratio or the Fermi energy, paving the way for future studies on various exotic magnetic textures formed on a quasiperiodic lattice through the e/a ratio.

DOI: 10.1103/PhysRevLett.130.176701

Quasicrystals (QCs) are solids that are characterized by long-range positional order with crystallographically forbidden symmetries such as fivefold, 10-fold, and 12-fold rotational symmetries. Since the first discovery of icosahedral QCs (*i* QCs) in 1984 [1], significant attention has been paid to the physical properties intrinsic to the quasiperiodicity of *i* QCs. In particular, the magnetism of QCs has been extensively studied to discover the first quasiperiodic arrangement of the order parameter, that is, magnetic moments. During the past quarter-century, various *i* QCs containing rare-earth (*R*) elements, such as Zn-Mg-*R* [2–9], Cd-Mg-*R* [10–12], and Cd-*R* *i* QCs [13,14] have been discovered. Moreover, researchers have paid immense attention to these *R*-bearing *i* QCs containing well-localized magnetic moments. However, no magnetic order but only spin-freezing phenomena were observed in these compounds, indicating a strongly frustrated nature of spins in *i* QCs. To date, the reason for this observation has not been well understood.

For nearly four decades, antiferromagnetism and other long-range magnetic orders such as ferro or ferrimagnetism were not observed in *i* QCs. Recently, ferromagnetic order was discovered in the Au-Ga-Gd and Au-Ga-Tb *i* QCs prepared using the melt-spinning method [15]. However, these *i* QCs are not suitable for investigations on their ferromagnetism (such as reported in the present work) because they contain a considerable amount of secondary 1/1 approximant crystal (AC) phase, which is also magnetic and needs to be eliminated for further investigation about their intrinsic magnetism. Given the metastable nature of the Au-Ga-(Gd,Tb) *i* QCs, removing the impurity phase from the structure through a heat treatment process is not plausible, making highly pure magnetic *i* QCs as a central and urgent issue in the magnetism research on *i* QCs. To solve this issue, herein, we report successful synthesis of ferromagnetic *i* QC with not only high phase purity but also largely tunable Au/Ga ratio in the Au-Ga-Dy system inside the ferromagnetic regime recently established for ACs [16].

For synthesis, mother alloys in the Au-Ga-Dy system containing 62–68 at. % Au and a constant Dy content of 15 at. % were prepared using arc-melting technique. The alloys were then subjected to rapid quenching onto a Cu wheel rotating at 4000 rpm. Powder x-ray diffraction (Rigaku MiniFlex600, Cu $-$ $K\alpha$) and scanning electron microscopy (SEM, JEOL JSM-IT100) equipped with an energy dispersive x-ray (EDX) spectrometer were utilized to study phase purity, and local compositions of the prepared polycrystalline compounds. Figure S1 in the Supplemental Material [17] shows a SEM backscattered image from a surface of as-quenched $Au_{62}Ga_{23}Dy_{15}$ *i* QC where a fairly single phase is observed. The dc magnetic susceptibility under zero-field-cooled (ZFC) and field-cooled (FC) modes (temperature range of 1.8–300 K and external dc fields up to 7×10^4 Oe) and specific heat were measured using superconducting quantum interference devices (Quantum Design, MPMS, and PPMS, respectively). Furthermore, selected area electron diffraction (SAED) patterns were acquired from $Au_{65}Ga_{20}Dy_{15}$ *i* QC using transmission electron microscopy (TEM, JEM-2010F).

Figure 1 shows powder x-ray diffraction (XRD) patterns of the $Au_xGa_{85-x}Dy_{15}$ ($x = 62$–68) *i* QCs. Herein, the Elser's indexing scheme [18] was used for indexing the *i* QC peaks. In the patterns, most of the peaks can be indexed as *i* QC peaks suggesting formation of single-phase

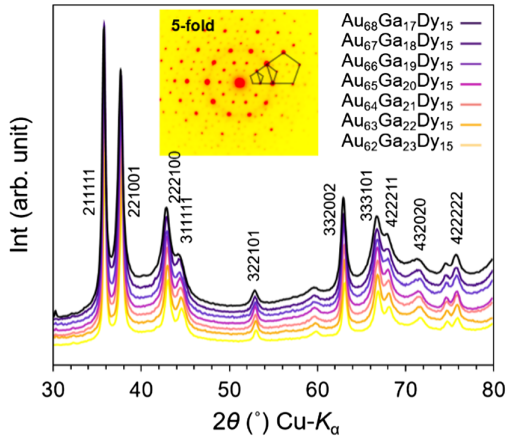

FIG. 1. Powder X-ray diffraction patterns of the $Au_xGa_{85-x}Dy_{15}$ x = 62–68 *i* QCs. In all the patterns, the peaks are indexed as those of a primitive *i* QC indicating formation of highly pure *i* QCs. The inset displays selected-area electron diffraction (SAED) pattern of the $Au_{65}Ga_{20}Dy_{15}$ *i* QC along the fivefold axis.

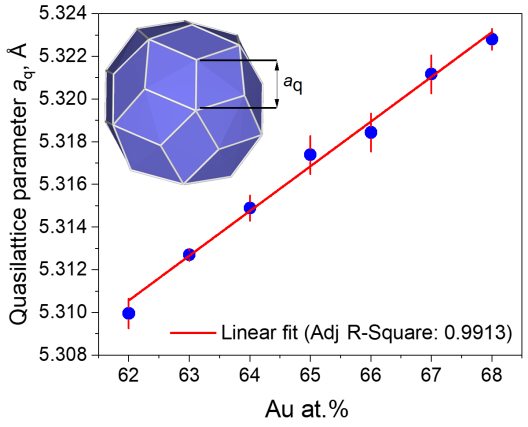

FIG. 2. Variation of quasilattice parameter a_q as a function of Au concentration in the rapidly quenched $Au_xGa_{85-x}Dy_{15}$ (x = 62–68) samples. The a_q values are obtained by averaging the estimates from (211111), (221001), and (332002) peaks in each sample.

i QCs. The inset of Fig. 1 shows SAED pattern of the $Au_{65}Ga_{20}Dy_{15}$ *i* QC with incidence axis along the fivefold rotational symmetry where the existence of the icosahedral symmetry unique to *i* QCs is evidenced. The τ scaling feature observed in the pattern indicates that the obtained *i* QC is a primitive one and is identical to the prototype *i* $Cd_{5.7}Yb$ [19].

Figure 2 shows variation of the quasilattice parameter a_q, defined as an edge length of the rhombic triacontahedron building unit in the *i* QC structure [19], as a function of Au concentration in the $Au_xGa_{85-x}Dy_{15}$ (x = 62–68) samples. Here, the a_q values were obtained by averaging the estimates from (211111), (221001), and (332002) peaks in each sample. The figure clearly shows a linear correlation between the a_q and the nominal Au content indicating a mutual substitution of Ga by Au in the samples, which is also evident from the SEM-EDX elemental analysis provided in Table S1 in the Supplemental Material [17]. Figure S2 plots nominal versus analyzed Au content of the *i* QCs where a fair consistency between the two can be inferred [17].

The results of high-temperature inverse magnetic susceptibility measurements of the Au-Ga-Dy *i* QCs under 1000 Oe are presented in Fig. S3 [17]. In the paramagnetic region, the magnetic susceptibility follows the Curie-Weiss law expressed as $\chi = N_A\mu_{\text{eff}}^2/3k_B(T\text{-}\theta_p)$ where N_A, k_B, and θ_p represent the Avogadro number, Boltzmann constant, and Weiss temperature, respectively. The effective magnetic moments μ_{eff} are in the range of 10.79–11.07μ_B, which are in good agreement with the theoretical value of a Dy^{3+} free ion (10.63μ_B). This indicates that the magnetic moments are well localized on the Dy^{3+} ions, similar to other *R*-containing *i* QCs.

Figure 3 shows low-temperature FC magnetic susceptibility defined as M/H of the $Au_xGa_{85-x}Dy_{15}$ (x = 62, 65, and 68) *i* QCs under 100 Oe where a rise below T_C (estimated from the minimum of the dC_p/dT curves with C_p being specific heat) indicates ferromagnetic behavior in the present Au-Ga-Dy *i* QCs. A relatively broad transition is commonly noticed in the present *i* QCs [which has also been observed in the Au-Ga-(Gd/Tb) *i* QCs [15]], which may be a characteristic feature of the ferromagnetic *i* QCs. A full set of FC and ZFC curves for the studied materials are provided separately in Fig. S4 (Supplemental Material [17]), where a deviation between the FC and ZFC susceptibilities is observed below T_C. This observation is similar to those for non-Heisenberg ferromagnetic ACs [20,21], which is attributed to the pinning of magnetic domain walls during the FC process as a characteristic feature of ferromagnets. The inset of Fig. 3 shows C_p/T variation of the $Au_xGa_{85-x}Dy_{15}$ ($x = 62$, 65, and 68) *i* QCs in the temperature range of 0–25 K.

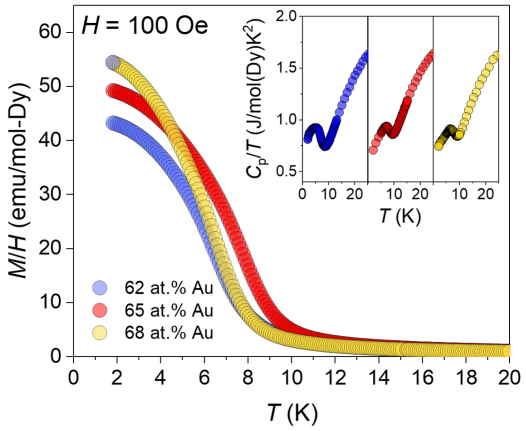

FIG. 3. Temperature dependence FC magnetic susceptibility (M/H) of the $Au_xGa_{85-x}Dy_{15}$ ($x = 62$, 65, and 68) i QCs. The inset shows C_p/T variation in the same samples as a function of temperature T in the range of 0–25 K.

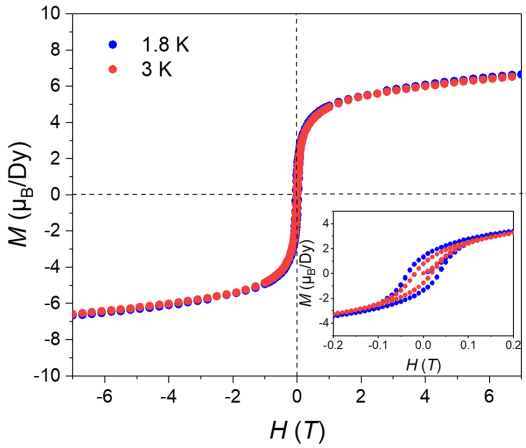

FIG. 4. M-H loop measured at $T = 1.8$ and 3 K both below the transition temperature $T_C = 7.5$ K in the $Au_{65}Ga_{20}Dy_{15}$ i QC. The inset shows magnified view from −0.2 and 0.2 T wherein a hysteresis loop can be observed.

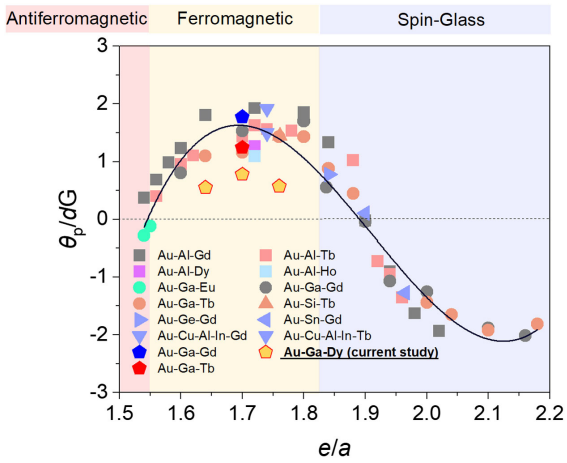

FIG. 5. Variation of normalized Weiss temperature, θ_p/dG, as a function of the electron-per-atom (e/a) ratio over a wide e/a range between 1.5 and 2.2 for the Au-based Tsai-type ACs along with newly discovered Au-Ga-Dy i QCs. The values obtained for the present Au-Ga-Dy i QCs are represented by yellow pentagon symbols in the figure. The θ_p/dG values of the present Au-Ga-Dy i QCs have a peak at $e/a = 1.70$, which well coincides with the peak of the polynomial fitting in the ACs.

The C_p/T curves clearly show sharp anomalies, which correspond well with the increase in M/H at T_C and verifies the occurrence of ferromagnetic transition. Further, the field dependence magnetization $(M - H)$ curve was measured at 1.8 and 3 K for the $Au_{65}Ga_{20}Dy_{15}$ i QC up to 7 T, the results of which is shown in Fig. 4. The magnitude of M at 1.8 K is suppressed to ∼6.9 μ_B/Dy^{3+}, approximately two-thirds of the full moment of a free Dy^{3+} ion ($gJ\,\mu_B = 10\ \mu_B/Dy^{3+}$). Such a suppression behavior has been observed in non-Heisenberg ferromagnetic ACs [20,21] and is associated with the strong uniaxial anisotropy for the R^{3+} spins with nonzero orbital angular momentum L. In addition, the $M - H$ loop of the $Au_{65}Ga_{20}Dy_{15}$ i QC in the inset of Fig. 4 clearly shows hysteresis behavior indicating the existence of spontaneous magnetization below T_C, which is also a characteristic feature of ferromagnets. Moreover, for the $Au_{65}Ga_{20}Dy_{15}$ i QC, the increase in remanence magnetization and coercivity by decreasing the temperature from T_C is consistent with the development of spontaneous magnetization below T_C. It is worth noting that both bifurcation between ZFC and FC curves and not fully saturating magnetization behavior at 7 T reflect the existence of the crystalline-electric-field (CEF) anisotropy in the present i QCs. Under the presence of the CEF anisotropy at the rare earth sites, the magnetic structure becomes noncollinear and noncoplanar, as reported elsewhere [20]. Therefore, the present ferromagnetic order may not be considered as a purely ferromagnetic, or a collinear ferromagnetic, but more like a noncoplanar ferrimagnetic one.

Figure 5 shows changes in the normalized Weiss temperature, θ_p/dG (dG being de Gennes factor defined as $(g_J - 1)^2 J(J + 1)$ where g_J and J denote the Landé g-factor and the total angular momentum, respectively), as a function of the electrons-per-atom (e/a) ratio over a wide e/a range of 1.5–2.2 for all the R-containing Au-based Tsai-type ACs reported to date [16,20,22–27] as well as the present Au-Al-Dy i QCs (represented by yellow pentagon symbols). Interestingly, the Weiss temperatures obtained from the present Au-Ga-Dy i QCs accords well with the polynomial fitting curve in the θ_p/dG versus e/a plot derived from other Au-based ACs. Moreover, the θ_p/dG values obtained from the $Au_xGa_{85-x}Dy_{15}$ ($x = 62, 65$, and 68) i QCs exhibit a maximum at $e/a = 1.70$, whose position also coincides with that observed for the ACs. This observation coherently confirms that the strongest ferromagnetic interaction occurs at $e/a = 1.\ 70$ for the Au-Ga-Dy i QC.

Next, we discuss the critical behavior of the Au-Ga-Dy i QC based on the scaling principle where the following equations hold near T_C [28].

$$M_s(T) = M_0(-\epsilon)^{\beta}; \qquad \epsilon < 0; \qquad T < T_c, \tag{1}$$

$$(H/M)_0(T) = (h_0/M_0)\epsilon^{\gamma}; \qquad \epsilon > 0; \qquad T > T_c, \tag{2}$$

where ϵ denotes the reduced temperature $(T - T_c)/T_c$ and M_0, h_0 are critical amplitudes. In the above equations, the critical exponent β is correlated with the spontaneous magnetization $M_s(T)$ at $H = 0$ below T_C while γ corresponds to initial inverse magnetic susceptibility $(H/M)_0(T)$ above T_C. Figure 6 shows the $M^{1/\beta} - (H/M)^{1/\gamma}$ plot of the $Au_{65}Ga_{20}Dy_{15}$ i QC (the notation modified Arrott plot is used for this plot) in the vicinity of T_C, where β and γ are determined as 0.54 and 0.89, respectively, on the basis of the scaling principle and Kouvel-Fisher (KF) equations [29] (refer to Supplemental Material and Figs. S5 and S6 for

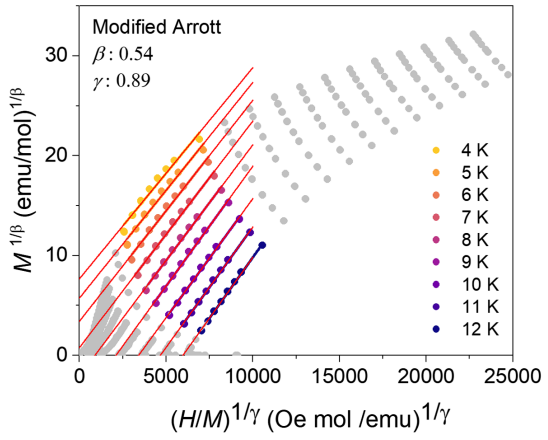

FIG. 6. The isotherms of $M^{1/\beta}$ vs $(H/M)^{1/\gamma}$ for $Au_{65}Ga_{20}Dy_{15}$ iQC where β and γ are 0.54 and 0.89, respectively. Nearly parallel linear behavior can be observed within the colored sections of the isotherms corresponding to magnetic fields of $0.4\ \mathrm{T} < H < 1.3\ \mathrm{T}$, with the lines of 7 and 8 K intercepting the $M^{1/\beta}$ axis at positive and negative values, respectively.

details [17]). In both analyses, an iteration has been performed by substituting the newly estimated β and γ values for the previous ones until convergence is obtained. In Fig. 6, nearly parallel linear behavior can be observed within the colored sections of the isotherms corresponding to magnetic fields of $0.4\ \mathrm{T} < H < 1.3\ \mathrm{T}$, with the lines of 7 and 8 K intercepting the $M^{1/\beta}$ axis at positive and negative values, respectively. The estimated T_C using the above methods (as described in the Supplemental Material [17]) is within a range of 7.45–7.48 K, which is in good agreement with the $T_c = 7.70$ K obtained from the C_p/T data confirming the consistency of the present analysis.

By comparing the estimated critical exponent $n(=\gamma/\beta) = 1.64$ for the present i QC to the three-dimensional (3D) universality classes: Landau mean-field model ($n = 2.00$) [30], the 3D Heisenberg model [30] ($n = 3.80$), the 3D Ising model [30] ($n = 3.82$), and the tricritical mean-field model [31] ($n = 4.00$), the obtained value ($n = 1.64$) is by far best explained by the Landau mean-field model indicating a mean-field-like nature of the ferromagnetic transition in the present i QC. The present results of $(\beta, \gamma) = (0.54, 0.89)$ are in agreement with $(\beta, \gamma) = (0.47, 1.12)$ deduced elsewhere [32] from bulk magnetization data in the Au-Si-Gd 1/1 AC. A noticeable difference between the two results relies in the value of γ [correlated with initial susceptibility $(H/M)_0$ [33]], which is lower in the present i QC than that of the Au-Si-Gd 1/1 AC [32]. Whether such a difference is due to the aperiodicity of the crystal structure is not clear at the moment and requires further systematic investigations, preferably on stable ferromagnetic i QCs that have not been discovered yet.

Further, we discuss the condition for the formation of the ferromagnetic QC in the present Au-Ga-Dy system. According to the Ruderman-Kittel-Kasuya-Yosida (RKKY) interaction theory [34], which is the major magnetic interaction between the R^{3+} spins of the R-containing QCs, the magnitude of the RKKY interaction scales with dG. As seen in Fig. 5, the magnetic-ground-state regime of the non-Heisenberg ACs changes from antiferromagnetic to ferromagnetic and then to spin glass with increasing e/a ratio. It is clearly seen that θ_p/dG depends on the e/a ratio of the ACs, depicting an oscillating universal curve. The θ_p value can be expressed as $\theta_p = \frac{1}{3}J(J+1)\sum_i n_i J_i$, where n_i is the number of ith nearest bonds with the interaction strength of J_i; therefore, θ_p can be regarded as a measure of the strength of the dominant magnetic interaction acting on each spin. It is expressed as $\theta_p = \frac{5}{3}J(J+1)(J_1 + J_2)$ for a single 12-spin icosahedron. In this respect, recently, the magnetic texture over the single 12-spin icosahedron was thoroughly investigated and a number of new nontrivial magnetic orders, such as hedgehog, anti-hedgehog, whirling, anti-whirling, and others, were identified with the simple variation in J_1/J_2 [35]. In the report, the sign change of θ_p is attributed to the sign change of J_i with the variation in the Fermi energy through the e/a ratio.

The e/a ratios of 1.64–1.76 in the present Au-Ga-Dy i QCs are situated inside the ferromagnetic regime of the ACs. An interesting observation here is that the magnetic order and the position of $\theta_{\max}$ of the i QC well coincide with those of ACs, validating the obtained $\theta_p - e/a$ diagram also for i QCs for the first time and confirming that the magnetic property of the i QCs is also tunable by varying the e/a ratio or the Fermi energy. Here, we note that Fermi energy is well defined in QCs since the energy eigenstates are, in principle, well defined [36], which is also true for amorphous materials (the electrons occupy the lowest energy eigenstates up to Fermi energy at zero Kelvin, in just the same manner as in periodic crystals). It is also noteworthy that the wave vector k is not a good quantum number in i QCs due to the lack of lattice periodicity, and the above description based on the RKKY interaction may be questionable for i QCs. Nonetheless, our observation shows that we can also control the balance of the ferromagnetic and the antiferromagnetic interactions by shifting the Fermi energy in i QCs in the same manner as in ACs, two prominently different long-range ordered materials. Our observation may suggest that the typical propagation length of a hole-electron pair created by localized magnetic moments is similar for QCs and ACs, which can be understood by considering that the QCs and ACs have the same local environment at a nanometer level. Both structures can be described as packing of the common rhombic triacontahedron (RTH) clusters with ~1.5 nm diameter. Further theoretical study along this line is certainly required to better understand the magnetism of QCs. Finally, our successful synthesis of composition-tunable ferromagnetic i QCs shows that e/a tuning is effective in controlling the QC magnetism and various exotic magnetic orders reflecting constituent spin

icosahedra can now be achieved by simply varying the e/a ratio. In this respect, the recent theoretical work shows that various noncoplanar spin configurations such as hedgehog (topological number: $Z = 1$), antihedgehog ($Z = -1$), whirling ($Z = 3$), and antiwhirling ($Z = -3$) magnetic textures are formed on the spin icosahedron in the ferromagnetic Tb-bearing i QC [37], which will provide unprecedented research topics in materials science, e.g., leading to various nontrivial physical properties such as anomalous and topological Hall effects in real i QCs.

This work was supported by the Japan Society for the Promotion of Science through Grants-in-Aid for Scientific Research (Grants No. JP19H05817, No. JP19H05818, No. JP19H05819, and No. JP21H01044) and JST, CREST Grant No. JPMJCR22O3, Japan.

*These authors contributed equally to this work.
†Corresponding author.
tamura@rs.tus.ac.jp

[1] D. Shechtman, I. Blech, D. Gratias, and J. W. Cahn, Phys. Rev. Lett. **53**, 1951 (1984).
[2] Y. Hattori, K. Fukamichi, K. Suzuki, A. Niikura, A. P. Tsai, A. Inoue, and T. Masumoto, J. Phys. Condens. Matter **7**, 4183 (1995).
[3] Y. Hattori, A. Niikura, A. P. Tsai, A. Inoue, T. Masumoto, K. Fukamichi, H. Arugakatori, and T. Goto, J. Phys. Condens. Matter **7**, 2313 (1995).
[4] B. Charrier and D. Schmitt, J. Magn. Magn. Mater. **171**, 106 (1997).
[5] Z. Islam, I. R. Fisher, J. Zarestky, P. C. Canfield, C. Stassis, and A. I. Goldman, Phys. Rev. B **57**, R11047 (1998).
[6] T. J. Sato, H. Takakura, A. P. Tsai, and K. Shibata, Phys. Rev. Lett. **81**, 2364 (1998).
[7] I. R. Fisher, K. O. Cheon, A. F. Panchula, P. C. Canfield, M. Chernikov, H. R. Ott, and K. Dennis, Phys. Rev. B **59**, 308 (1999).
[8] T. J. Sato, H. Takakura, A. P. Tsai, K. Shibata, K. Ohoyama, and K. H. Andersen, Phys. Rev. B **61**, 476 (2000).
[9] J. Dolinsek, Z. Jaglicic, M. A. Chernikov, I. R. Fisher, and P. C. Canfield, Phys. Rev. B **64**, 224209 (2001).
[10] T. J. Sato, J. Q. Guo, and A. P. Tsai, J. Phys. Condens. Matter **13**, L105 (2001).
[11] T. J. Sato, H. Takakura, J. Q. Guo, A. P. Tsai, and K. Ohoyama, J. Alloys Compd. **342**, 365 (2002).
[12] S. E. Sebastian, T. Huie, I. R. Fisher, K. W. Dennis, and M. J. Kramer, Philos. Mag. **84**, 1029 (2004).
[13] A. I. Goldman, T. Kong, A. Kreyssig, A. Jesche, M. Ramazanoglu, K. W. Dennis, S. L. Bud'ko, and P. C. Canfield, Nat. Mater. **12**, 714 (2013).
[14] T. Kong, S. L. Budko, A. Jesche, J. McArthur, A. Kreyssig, A. I. Goldman, and P. C. Canfield, Phys. Rev. B **90**, 014424 (2014).
[15] R. Tamura, A. Ishikawa, S. Suzuki, A. Kotajima, Y. Tanaka, N. Shibata, T. Yamada, T. Fujii, C. Wang, M. Avdeev, K. Nawa, D. Okuyama, and T. J. Sato, J. Am. Chem. Soc. **143**, 19928 (2021).
[16] S. Suzuki, A. Ishikawa, T. Yamada, T. Sugimoto, A. Sakurai, and R. Tamura, Mater. Trans., JIM **62**, 298 (2021).
[17] See Supplemental Material at http://link.aps.org/supplemental/10.1103/PhysRevLett.130.176701 for sample characterization, temperature dependence of magnetic susceptibility and inverse magnetic susceptibility and calculation of β and γ on the basis of the scaling principle and Kouvel-Fisher equations.
[18] V. Elser, Phys. Rev. B **32**, 4892 (1985).
[19] H. Takakura, C. P. Gomez, A. Yamamoto, M. De Boissieu, and A. P. Tsai, Nat. Mater. **6**, 58 (2007).
[20] T. Hiroto, K. Tokiwa, and R. Tamura, J. Phys. Condens. Matter **26**, 216004 (2014).
[21] G. H. Gebresenbut, M. S. Andersson, P. Nordblad, M. Sahlberg, and C. P. Gomez, Inorg. Chem. **55**, 2001 (2016).
[22] P. Kozelj, S. Jazbec, S. Vrtnik, A. Jelen, J. Dolinsek, M. Jagodic, Z. Jaglicic, P. Boulet, M. C. de Weerd, J. Ledieu, J. M. Dubois, and V. Fournée, Phys. Rev. B **88**, 214202 (2013).
[23] T. Hiroto, G. H. Gebresenbut, C. P. Gomez, Y. Muro, M. Isobe, Y. Ueda, K. Tokiwa, and R. Tamura, J. Phys. Condens. Matter **25**, 426004 (2013).
[24] A. Ishikawa, T. Hiroto, K. Tokiwa, T. Fujii, and R. Tamura, Phys. Rev. B **93**, 024416 (2016).
[25] A. Ishikawa, T. Fujii, T. Takeuchi, T. Yamada, Y. Matsushita, and R. Tamura, Phys. Rev. B **98**, 220403(R) (2018).
[26] S. Yoshida, S. Suzuki, T. Yamada, T. Fujii, A. Ishikawa, and R. Tamura, Phys. Rev. B **100**, 180409(R) (2019).
[27] K. Inagaki, S. Suzuki, A. Ishikawa, T. Tsugawa, F. Aya, T. Yamada, K. Tokiwa, T. Takeuchi, and R. Tamura, Phys. Rev. B **101**, 180405(R) (2020).
[28] H. E. Stanley, *Introduction to Phase Transitions and Critical Phenomena* (Oxford University Press, Oxford, 1971), p. 175.
[29] J. S. Kouvel and M. E. Fisher, Phys. Rev. **136**, 1626 (1964).
[30] A. Arrott, Phys. Rev. **108**, 1394 (1957).
[31] S. K. Banerjee, Phys. Lett. **12**, 16 (1964).
[32] T. Shiino, G. H. Gebresenbut, C. P. Gómez, U. Häussermann, P. Nordblad, A. Rydh, and R. Mathieu, Phys. Rev. B **106**, 174405 (2022).
[33] B. Widom, J. Chem. Phys. **43**, 3898 (1965).
[34] K. Yosida, Phys. Rev. **106**, 893 (1957).
[35] S. Suzuki, R. Tamura, and T. Sugimoto, Mater. Trans., JIM **62**, 367 (2021).
[36] Y. Ishii and T. Fujiwara, J. Alloys Compd. **342**, 343 (2002).
[37] S. Watanabe, Sci. Rep. **11**, 17679 (2021).